Cosmological history and direct detection of QCD axion

Yue Zhao

HKUST

e-Print: 2506.19918 [hep-ph]
e-Print: 2511.14851 [hep-ph]

Current Status of Particle Physics:

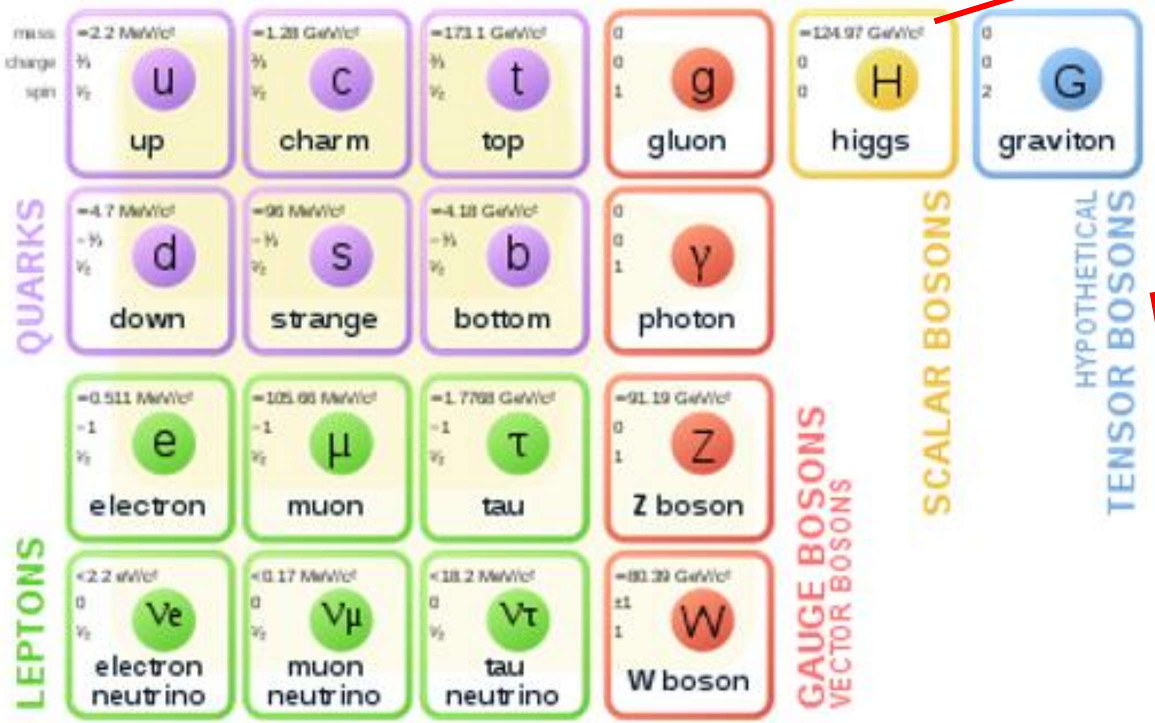

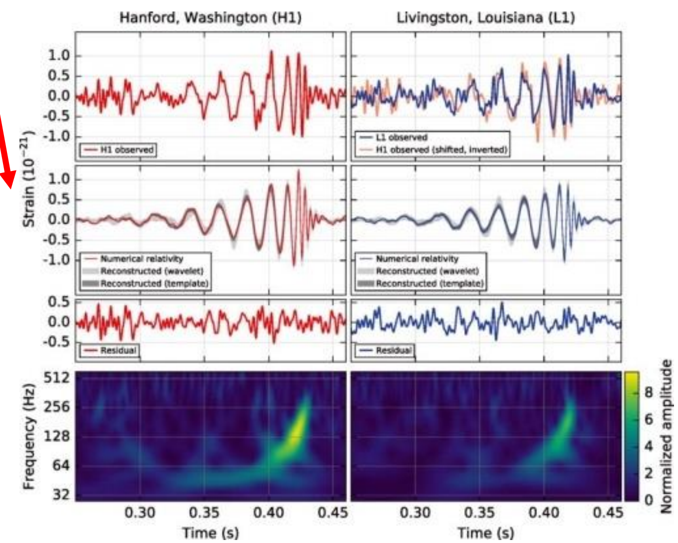

+ anything else?

Left-over problems:

- The identity of dark matter
- Gauge hierarchy problem
- Strong CP problem
- The identity of inflaton field
- Baryogenesis
- Cosmological constant

⋮

Left-over problems:

- The identity of dark matter → misalignment mechanism
- Gauge hierarchy problem → relaxion
- Strong CP problem → QCD axion
- The identity of inflaton field
- Baryogenesis
- Cosmological constant

(The identity of inflaton field, Baryogenesis, Cosmological constant) } can be related to axion

•
•
•

Theory motivations:

Strong CP-problem:

$$(\theta - \mathrm{arg\ det\ M_q})\frac{\alpha_s}{8\pi}\mathrm{G\tilde{G}}$$

$$\bar{\theta} < 10^{-10}$$

Introduce axion field:

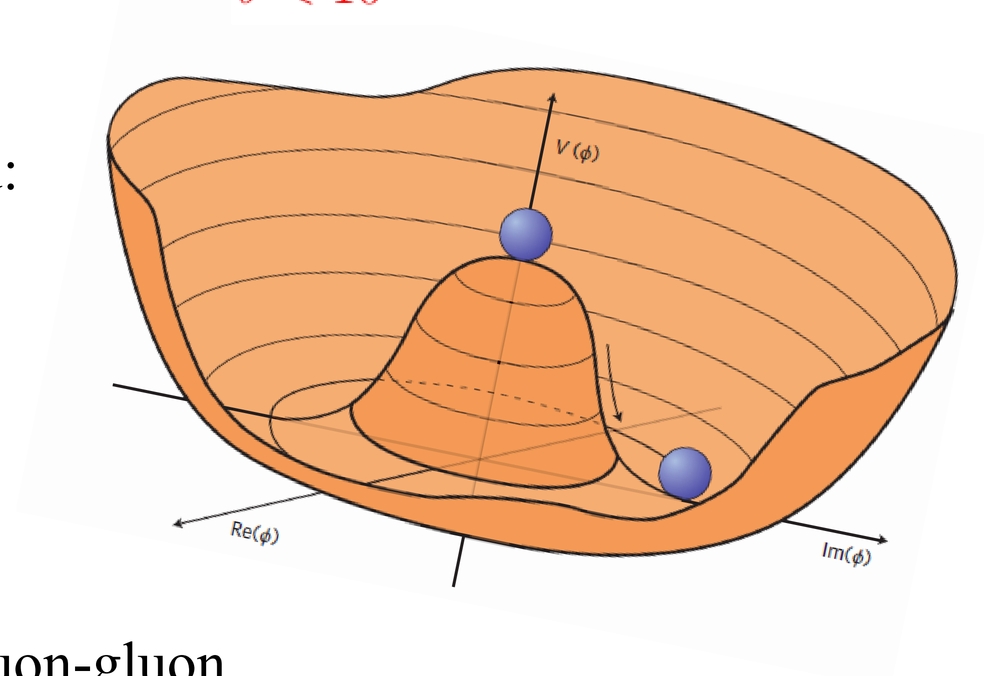

Couplings:

axion-gluon-gluon
axion-photon-photon
axion-fermion-fermion

Standard QCD axion thermal history

$$V(\theta_a, T) \equiv V(\theta_a) \times h(T) = -m_\pi^2 f_\pi^2 \sqrt{1 - \frac{4 m_u m_d}{(m_u + m_d)^2} \sin^2\left(\frac{\theta_a}{2}\right)} \times h(T)$$

$$h(T) = \begin{cases} 1 & T \leq T_{\rm QCD}\,, \\ \left(\frac{T_{\rm QCD}}{T}\right)^8 & T > T_{\rm QCD}\,. \end{cases}$$

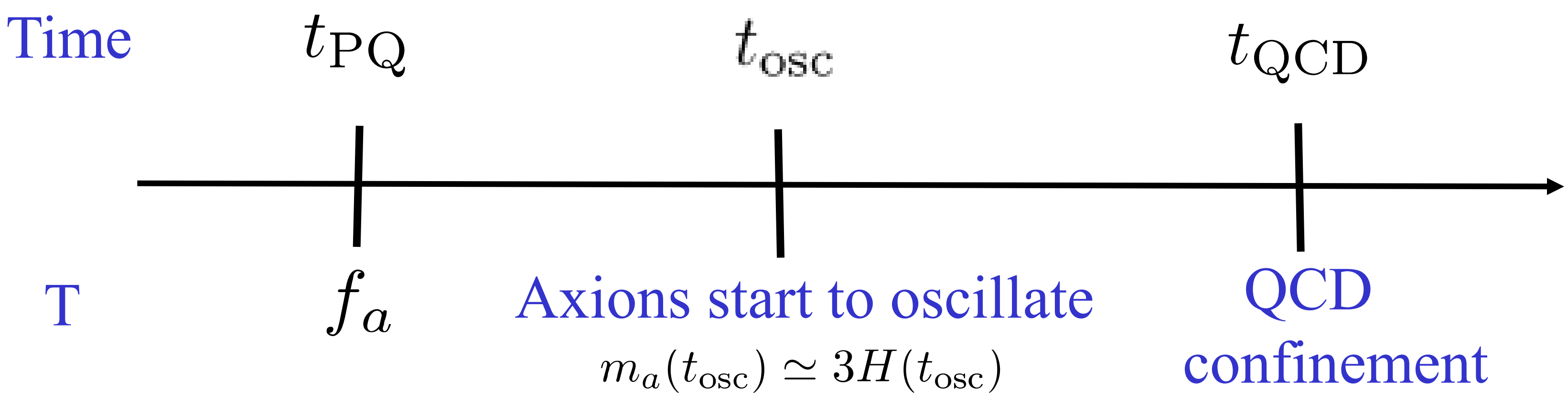

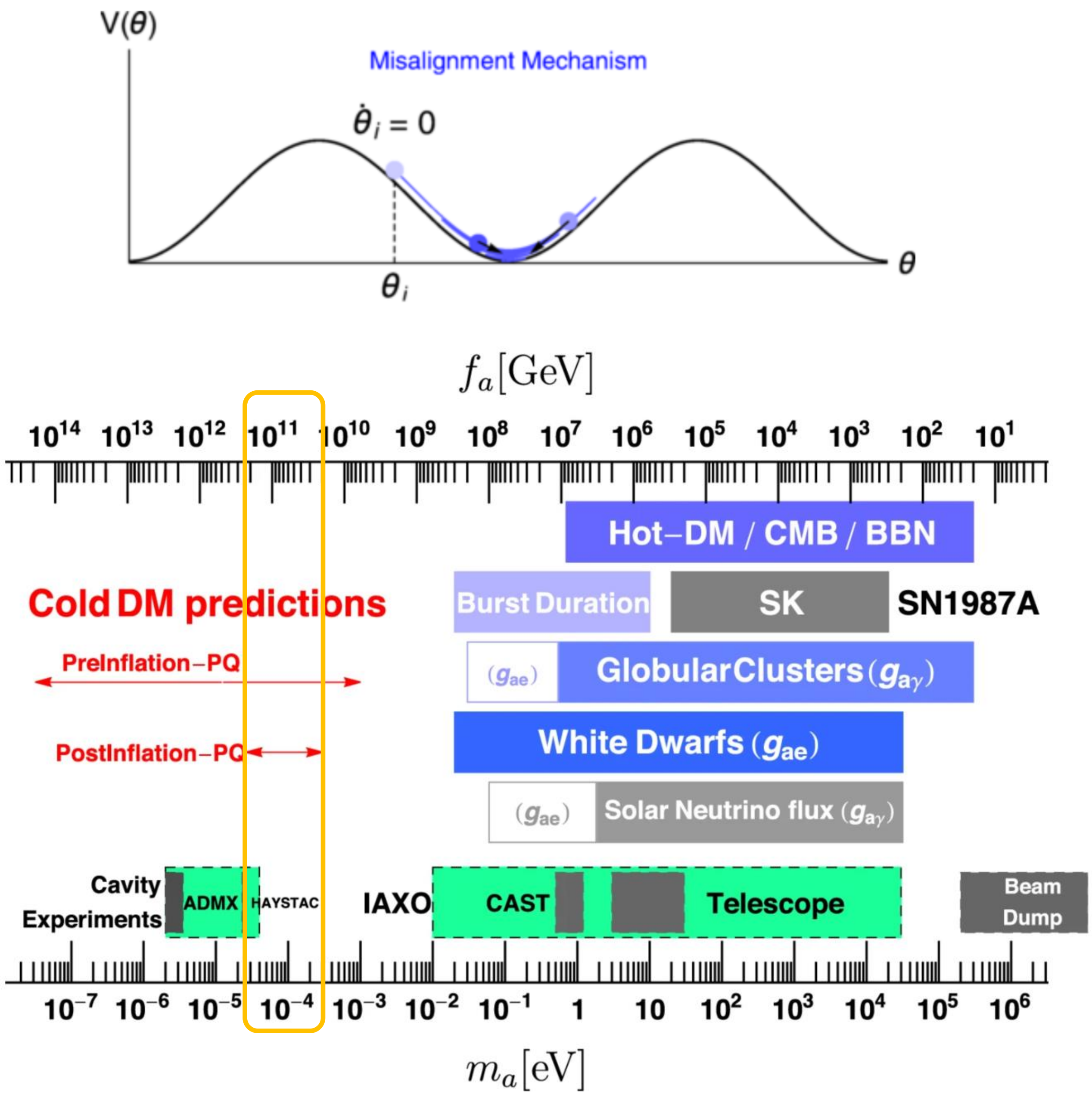

V(θ)
Misalignment Mechanism
$\dot{\theta}_i = 0$
θ_i
θ
f_a[GeV]
10^{14} 10^{13} 10^{12} 10^{11} 10^{10} 10^{9} 10^{8} 10^{7} 10^{6} 10^{5} 10^{4} 10^{3} 10^{2} 10^{1}
Hot−DM / CMB / BBN
Cold DM predictions
Burst Duration
SK
SN1987A
PreInflation−PQ
(g_{ae})
GlobularClusters ($g_{a\gamma}$)
PostInflation−PQ
White Dwarfs (g_{ae})
(g_{ae})
Solar Neutrino flux ($g_{a\gamma}$)
Cavity
Experiments
ADMX
HAYSTAC
IAXO
CAST
Telescope
Beam
Dump
10^{-7} 10^{-6} 10^{-5} 10^{-4} 10^{-3} 10^{-2} 10^{-1} 1 10 10^{2} 10^{3} 10^{4} 10^{5} 10^{6}
m_a[eV]

Kinetic Misalignment

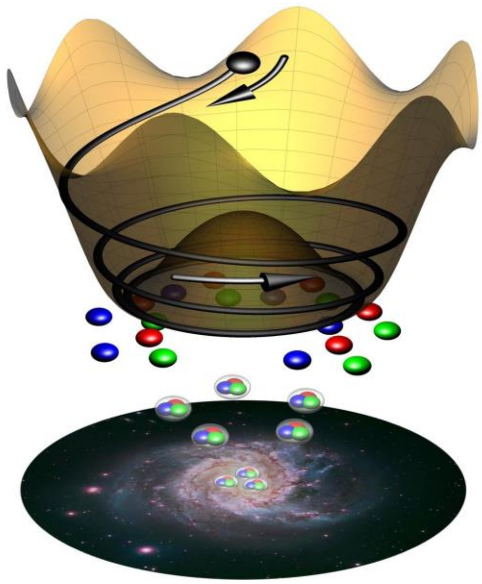

The kination era may change the prediction on the axion relic abundance.

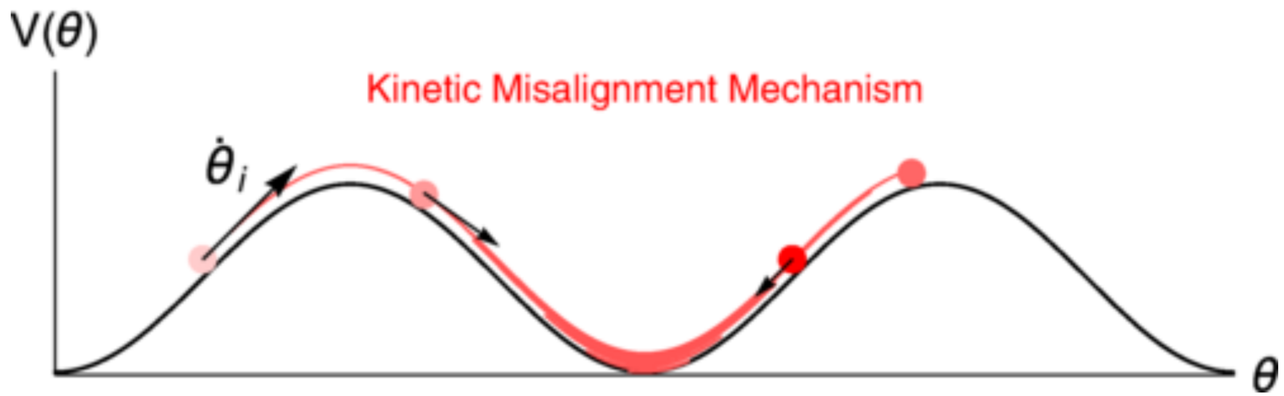

First Order Phase Transition

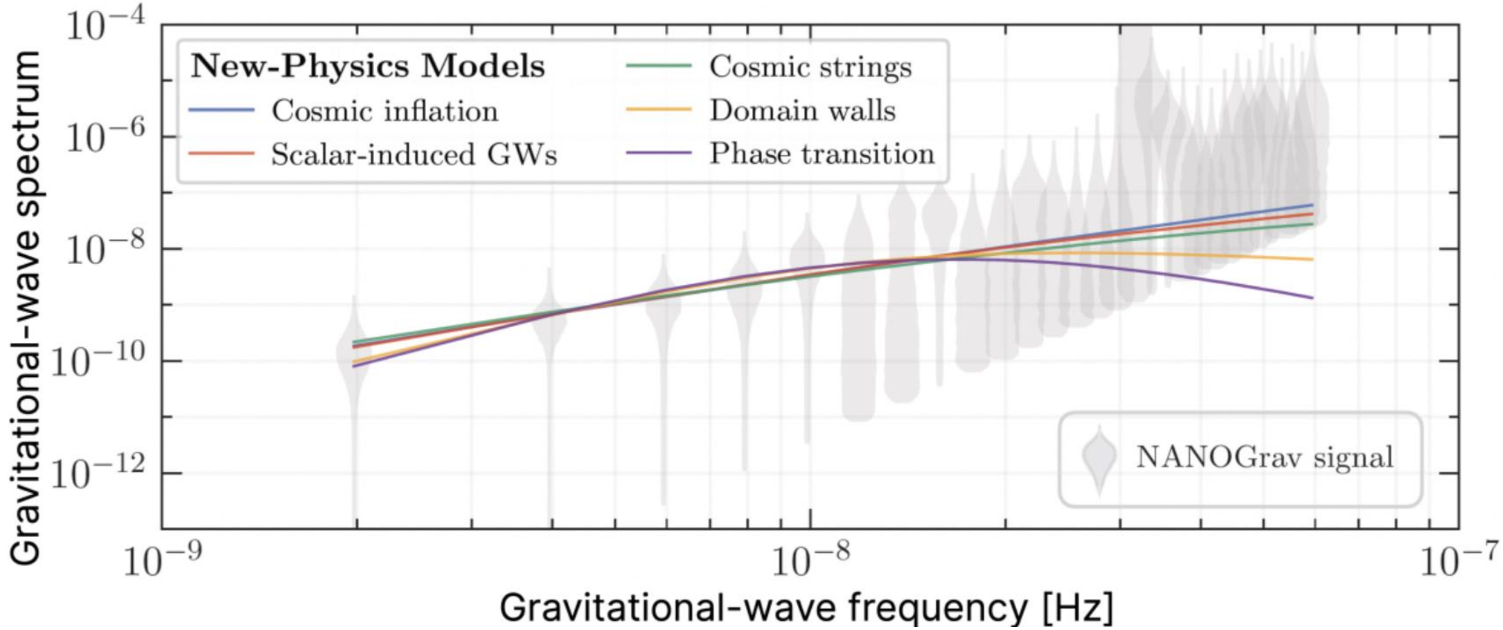

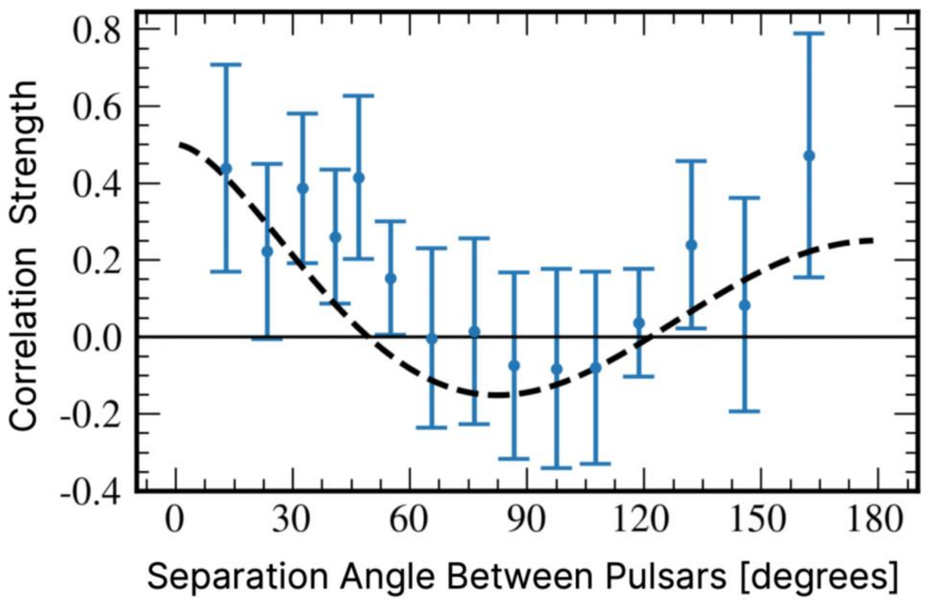

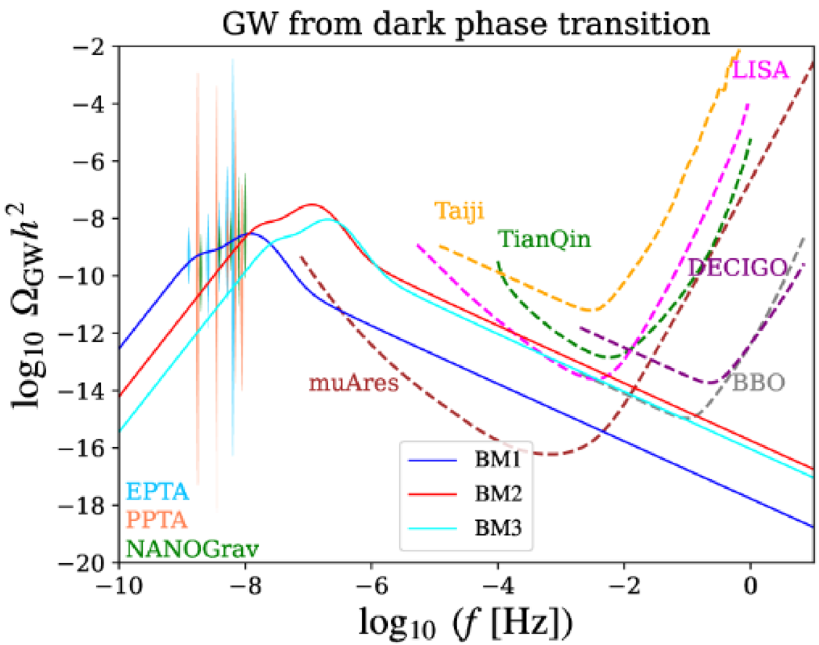

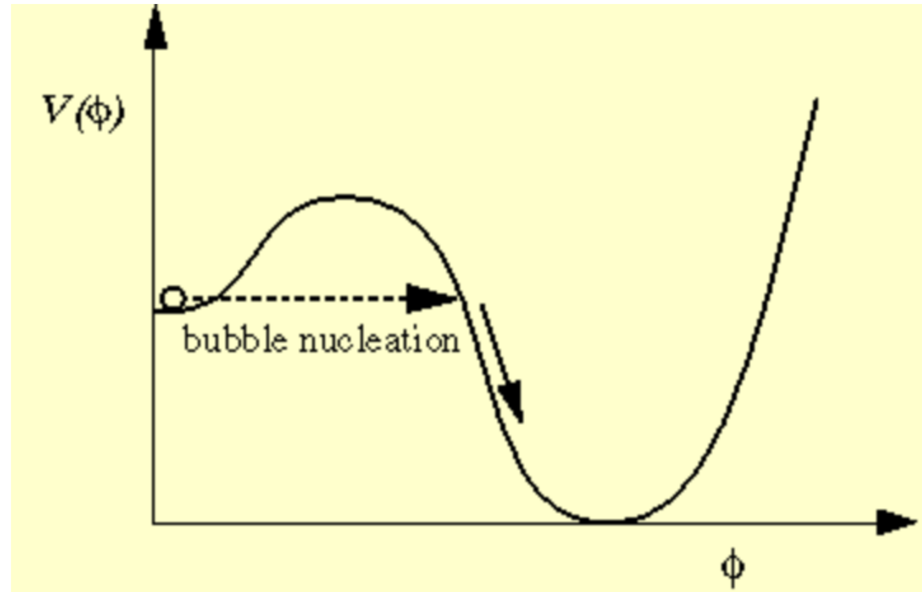

Strong FOPT @ O(QCD confinement scale).

Reheat the Universe significantly due to large latent heat release.

Modify the thermal history and may lead to interesting phenomena.

⇨ Reset axion DM relic abundance
Domain Wall production
⇨ May overclose the universe
May lead to interesting features of GW at higher frequency.

QCD axion history with the FOPT

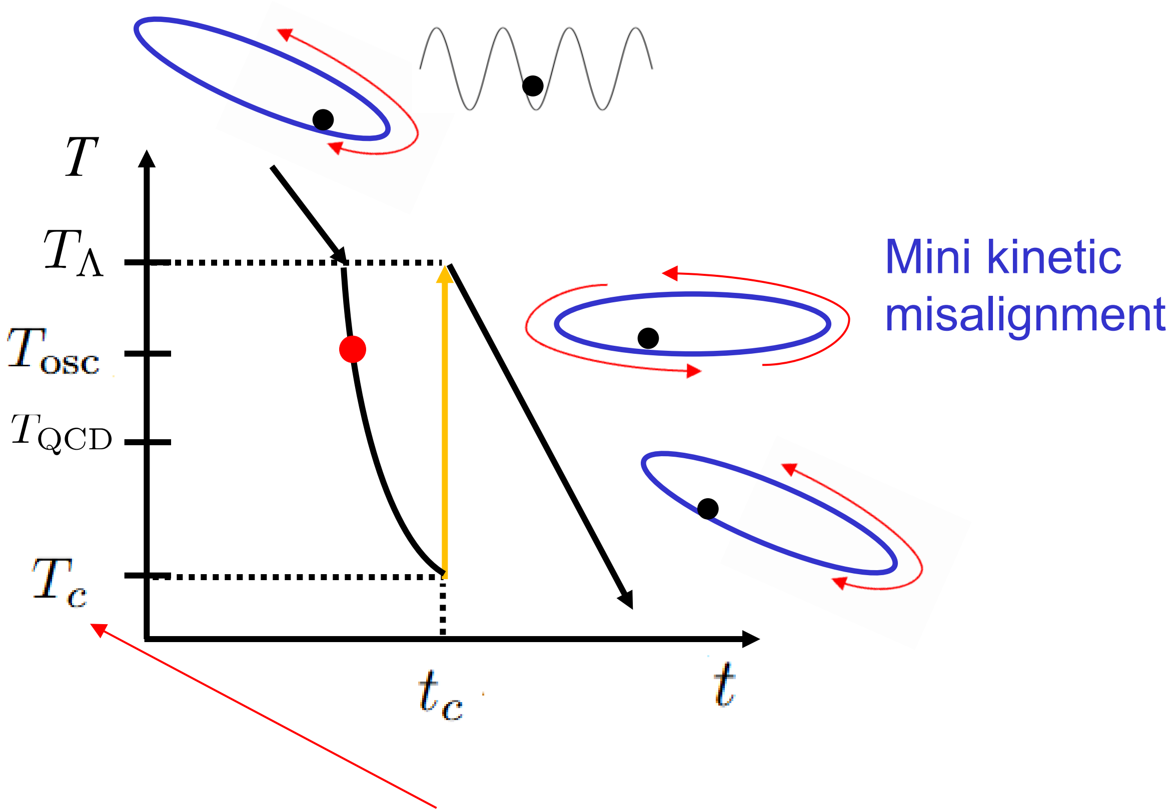

FOPT may happen at
O(10 MeV-GeV) regime.

Mini Kinetic Misalignment

Based on the WKB approximation, the ratio of the axion number density to the entropy density is conserved.

The axion field amplitude at the time of phase transition:

$$\theta_{a,\mathrm{PT}} = \theta_a(t = t_{\mathrm{PT}}) \simeq \theta_{a,i} \left(\frac{m_a(T_{\mathrm{osc}})}{m_a(T_{\mathrm{PT}})}\right)^{1/2} \left(\frac{T_{\mathrm{PT}}}{T_{\mathrm{osc}}}\right)^{3/2} \left(\frac{g_{*S}(T_{\mathrm{PT}})}{g_{*S}(T_{\mathrm{osc}})}\right)^{1/2} \boxed{\cos\phi_{\mathrm{PT}}} \,.$$

a random phase

$$K(T_\Lambda) = \dot{\theta}^2_{a,\mathrm{PT}} f_a^2/2 \qquad V_{\mathrm{max}}(T_\Lambda) = 2 f_a^2 m_a(T_\Lambda)^2$$

Mini kinetic misalignment occurs if

$$K(T_\Lambda) \gg V_{\mathrm{max}}(T_\Lambda)$$

QCD Axion evolution after FOPT

The reheating time scale (t_{reh}) after FOPT is model dependent.

If $t_{reh} > H_{PT}^{-1}$, the universe is reheated uniformly.

The evolution of the axion field remains the same spatially.

$$\ddot{\theta}_a + 3H(t)\dot{\theta}_a + m_a^2(t)\sin\theta_a = 0$$

When $K(T_\Lambda) \gg V_{\max}(T_\Lambda)$

$$\theta_a(t) = \theta_a(t_{\rm PT}) + \frac{\dot{\theta}_{a,\rm PT}}{H_\Lambda}\left[1 - \left(\frac{t_{\rm PT}}{t}\right)^{1/2}\right]$$

When $K(T_{\rm trap}) \simeq V_{\max}(T_{\rm trap})$, axion is trapped.

$$T_{\rm trap}/T_\Lambda = (K(T_\Lambda)/V_{\max}(T_\Lambda))^{-1/14}$$

6 from kinetic energy + 8 from potential raise

Resetting Misalignment

A reset of the misalignment is easily achieved.

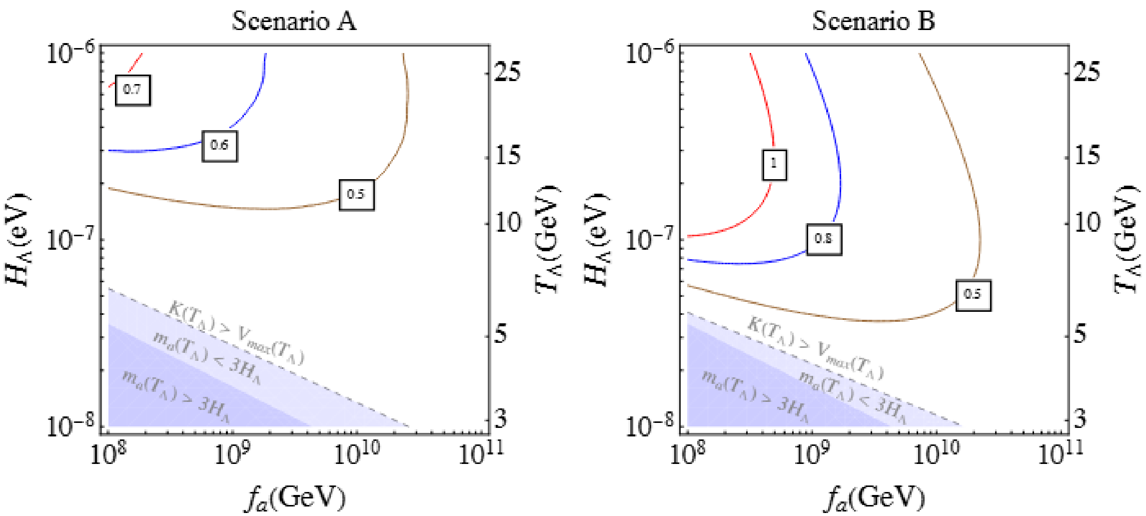

FIG. 2. The contours of the reset θ_a value. Here we choose $\theta_{a,i} = 0.2$ and $\sin\phi_{\rm PT} = 1/\sqrt{2}$. We also show the parameter space where the kinetic energy is unimportant, and the axion field oscillates as matter or is frozen after reheating.

Interesting implication to QCD axion relic abundance!

Inhomogeneity From Bubble Emergence

If reheating happens quickly,
inhomogeneous features are generated
lead to interesting phenomena

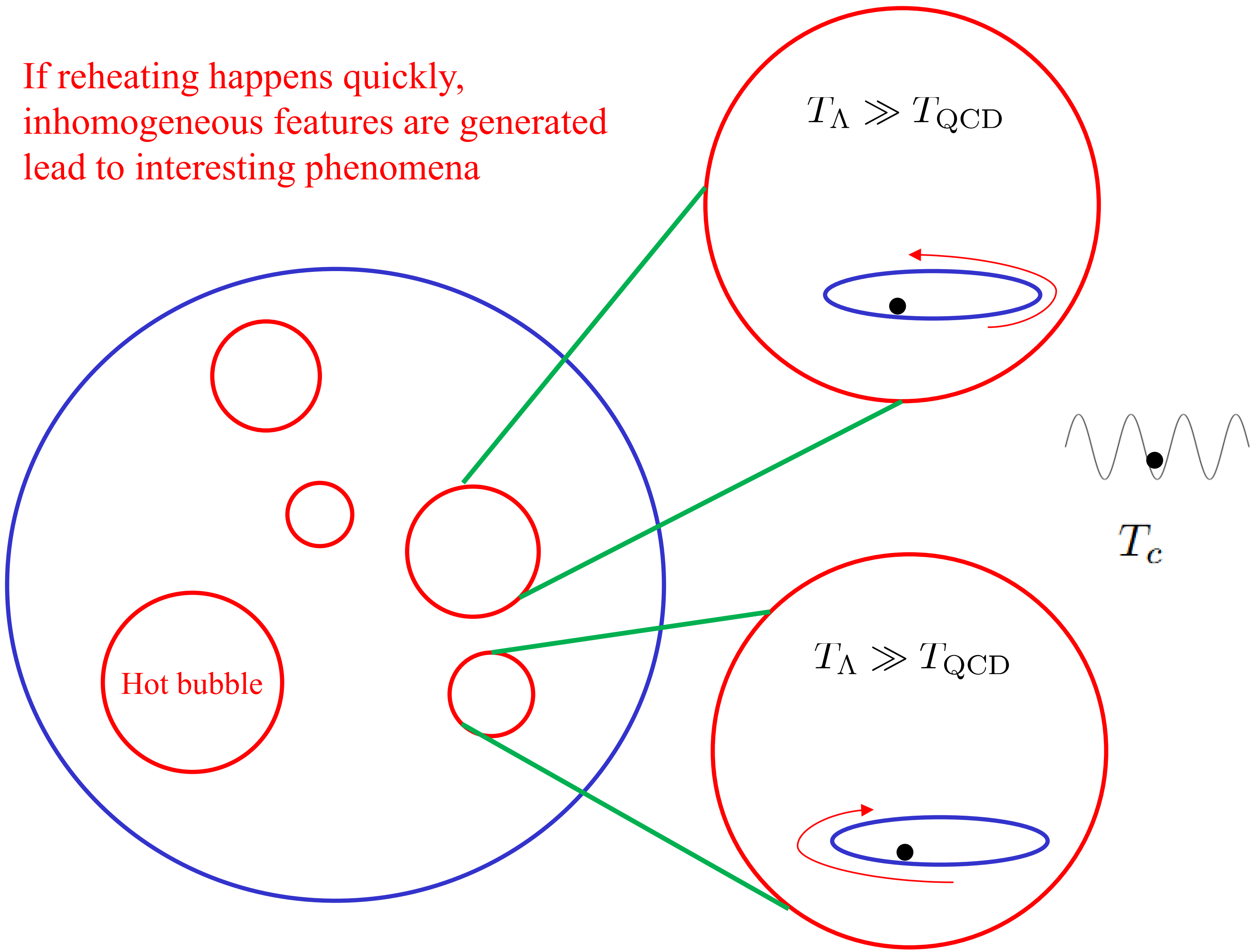

Inhomogeneity From Bubble Emergence

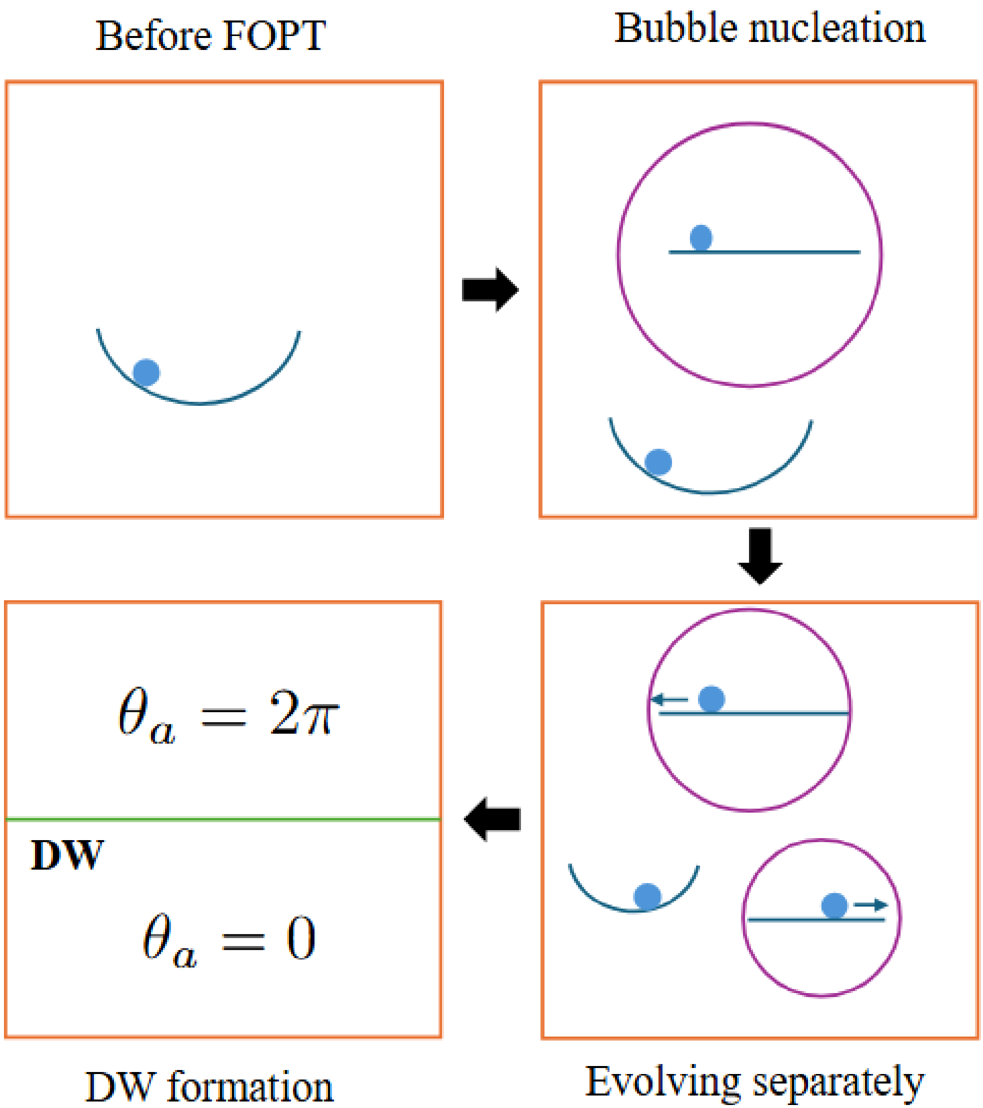

Inhomogeneity From Bubble Emergence

$$\ddot{\theta}_a + 3H\dot{\theta}_a - \frac{\nabla^2}{a(t)^2}\theta_a + m_a^2(T)\sin\theta_a = 0$$

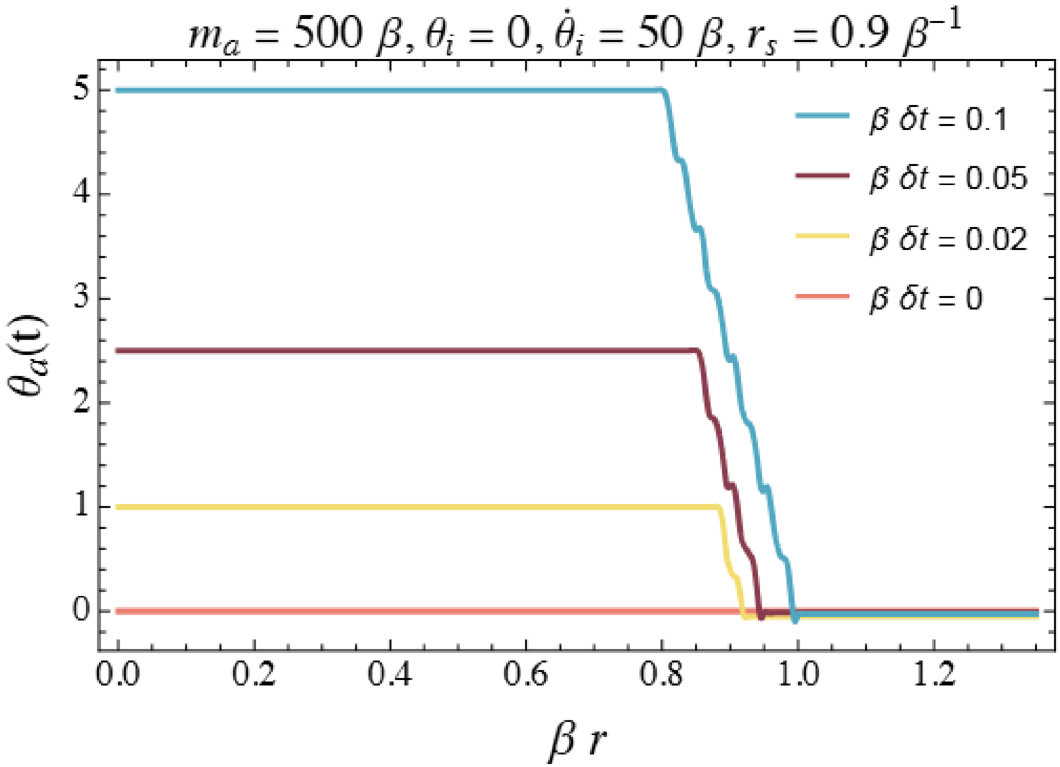

Reheating happens when the bubble is nearly to merge with other bubbles.

$$t_{reh} \sim (\beta H)^{-1}$$

Domain Wall Formation

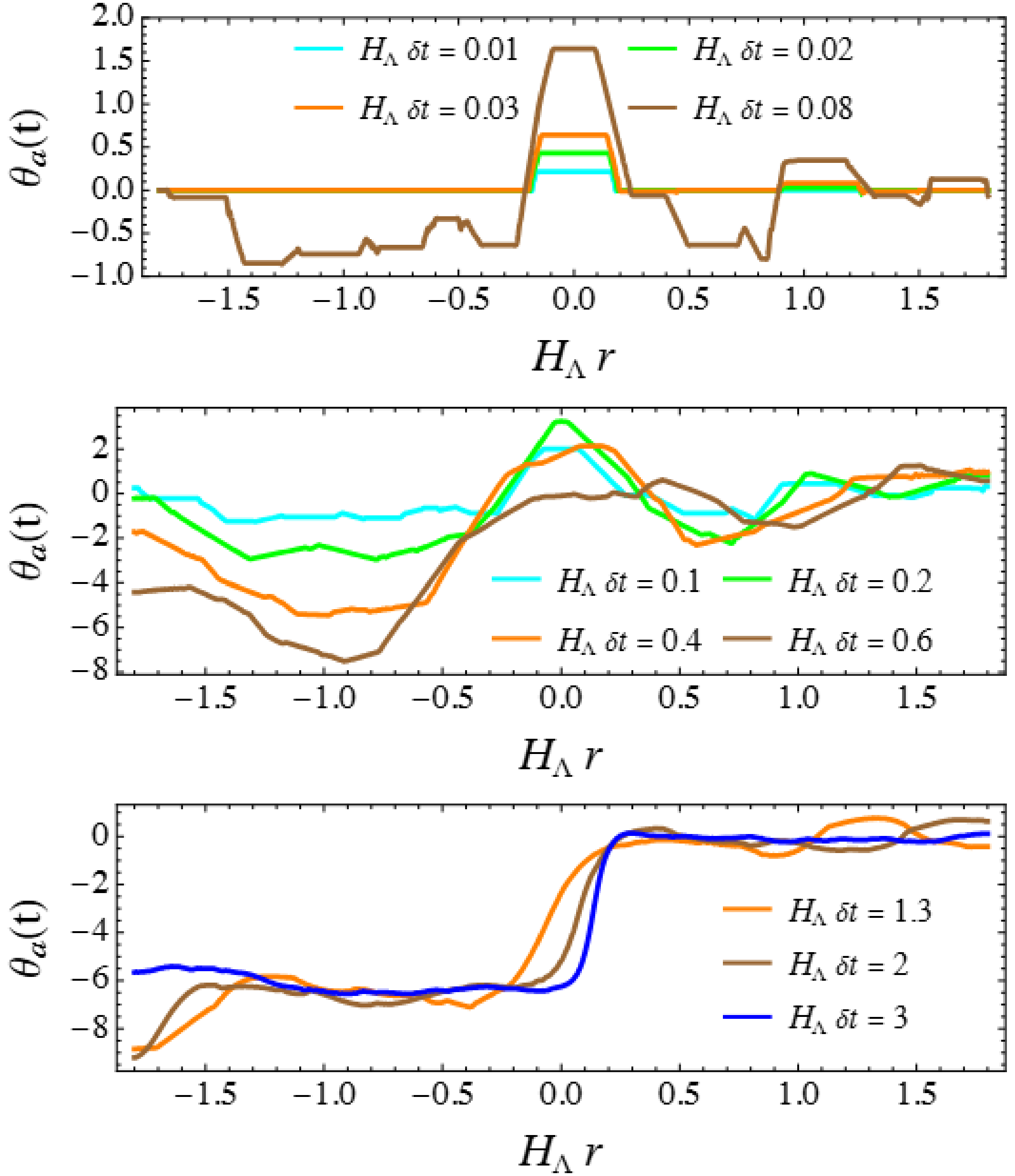

$m_a \sim 0$

m_a
non-negligible

trapped,
domain wall
formation

Domain Wall Formation

Condition for domain wall formation:

$$\frac{\dot{\theta}_{a,\mathrm{PT}}}{\beta}\left(\frac{T_{\mathrm{trap}}}{T_{\Lambda}}\right) > \pi$$

redshift factor

There is cosmic string produced, thus no boundary for DWs

Finite-sized enclosed domain walls:

Axion radiation from closed DWs.

Change in axion relic abundance.

Infinitely extended domain walls:

Percolation theorem: 31%

Scaling regime: $\rho_w \sim \sigma/t$

$m_{a,0} f_a^2 \sim \Lambda_{\mathrm{QCD}}^2 f_a \quad >> \quad 1\ \mathrm{MeV}^3$ overclose the universe

Domain Wall Formation

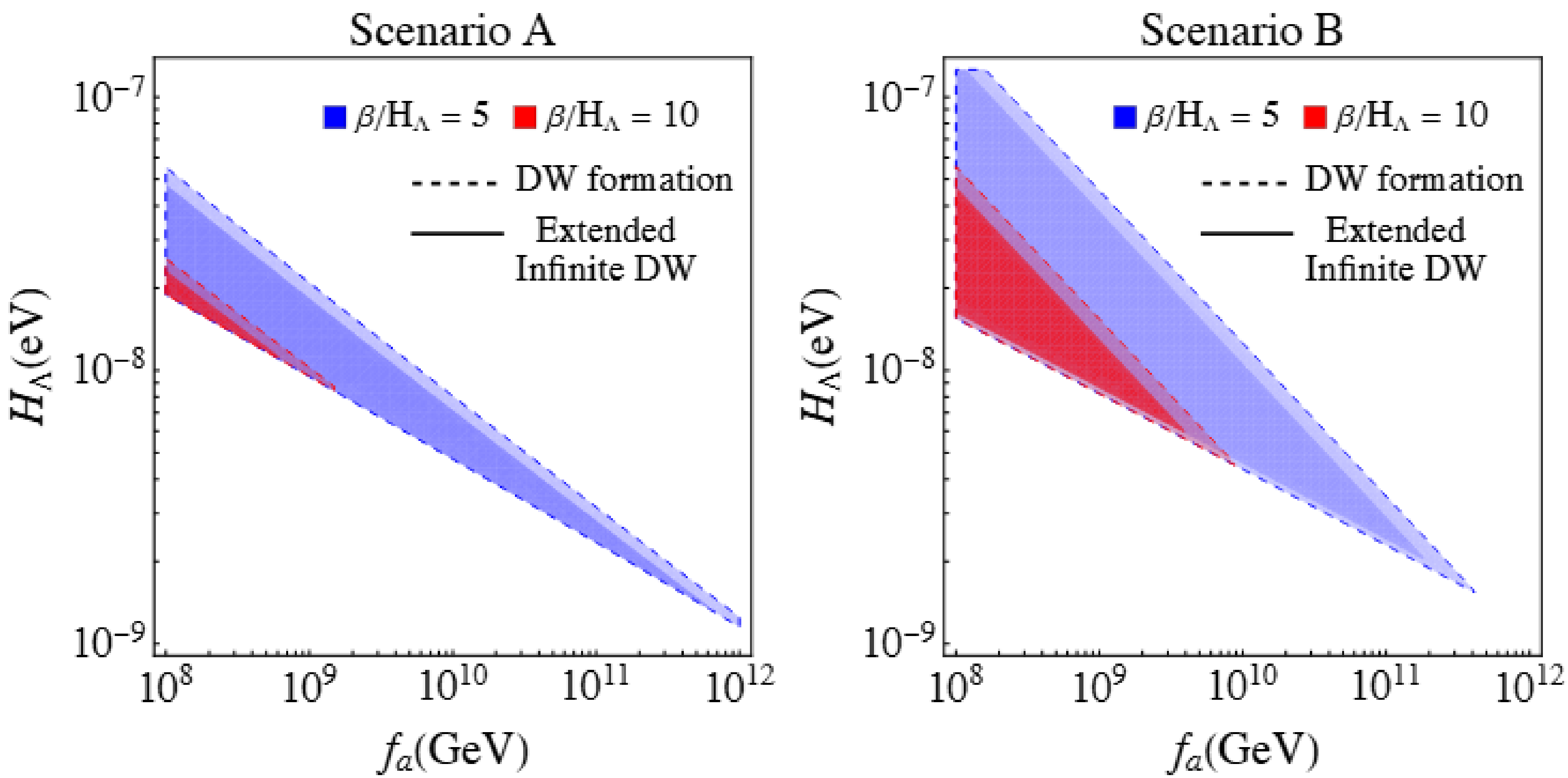

$$\theta_{a,i} = 2$$

Domain Wall Formation

Instantaneous reheating: $t_{reh} \ll (\beta H)^{-1}$

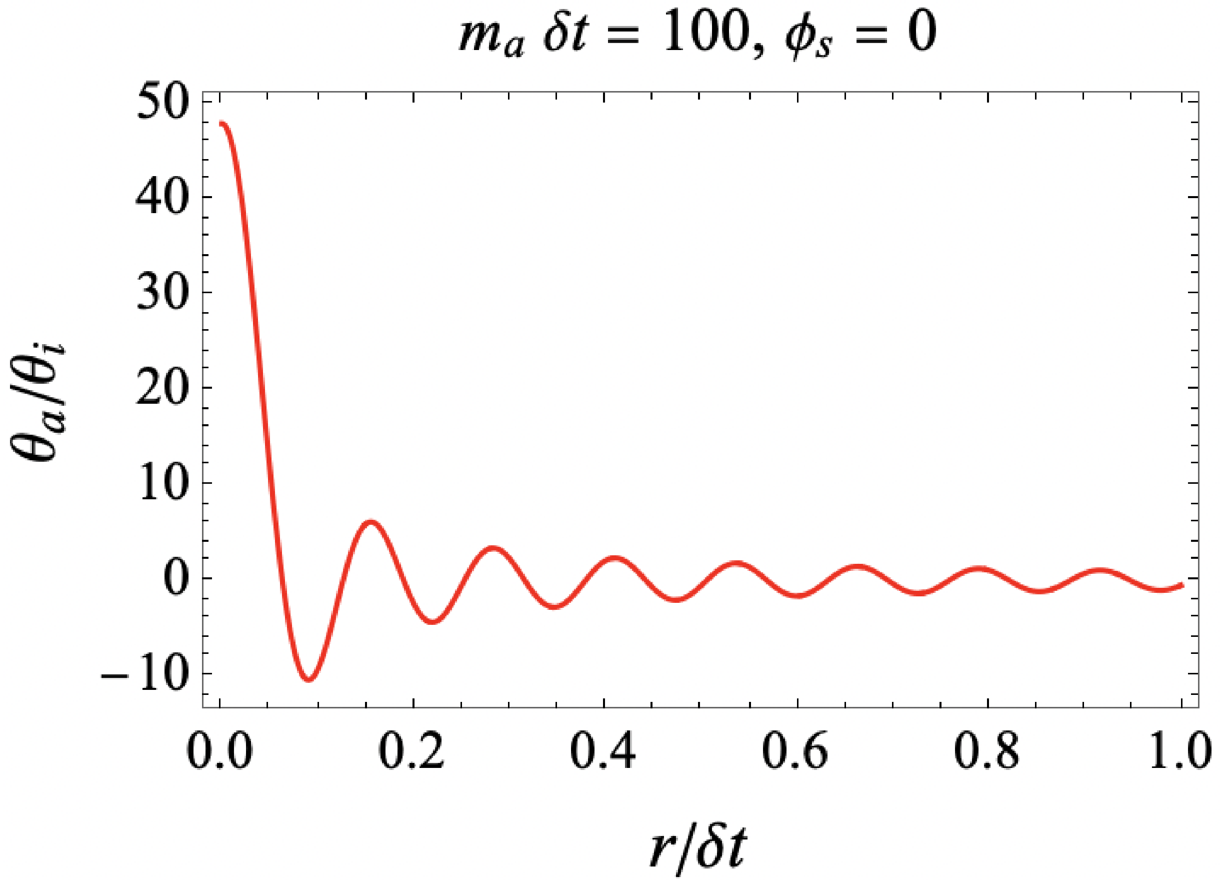

Only the center gains large field value.
Small enclosed bubbles are produced.

Conclusion 1

FOPT at QCD scale is hinted by NANOGrav.

The existence of QCD axion is very motivated.

⇨ Combining these two aspects leads to interesting cosmology!

Mini kinetic misalignment is a natural prediction.

Axion relic abundance is reset.

Domain wall formation, without cosmic strings, is expected.

⇨ Enclosed DWs decay away and change relic abundance.

Infinitely extended DWs easily overclose the universe.

QCD axion direct detection

$$\underbrace{(\theta - \mathrm{arg\ det\ M_q})}_{0}\frac{\alpha_s}{8\pi}\mathrm{G}\tilde{\mathrm{G}}$$

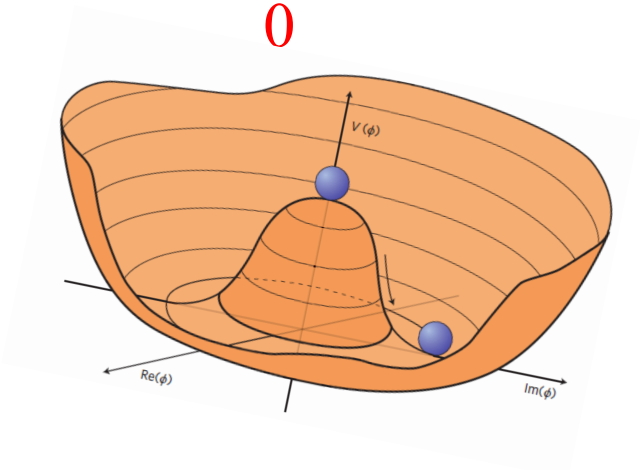

The introduction of axion sets the average value of $\bar{\theta}$ to zero.

Axion DM leads to a time dependent $\bar{\theta}$.

$$a(t,\vec{x}) \approx \frac{\sqrt{2\rho_{\mathrm{DM,local}}}}{m_a}\sin\left(\omega_a t - \vec{p}\cdot\vec{x}\right)$$

Chiral Lagrangian

Axion affects the nucleon and mesons through Chiral Lagrangian.

$$u \rightarrow e^{i\phi_u} u$$
$$d \rightarrow e^{i\phi_d} d,$$
$$\phi_u + \phi_d = \theta$$

$$(\theta - \arg\det \mathrm{M_q})\frac{\alpha_s}{8\pi}\mathrm{G}\tilde{\mathrm{G}}$$

lead to pion-axion mixing

$$U = e^{i\pi^a\tau^a/f_\pi} \qquad U_0 = \begin{pmatrix} e^{i\phi_u} & 0 \\ 0 & e^{i\phi_d} \end{pmatrix}$$

$$\mathcal{L} = -\frac{1}{4}f_\pi^2 \mathrm{Tr}[\partial_\mu U \partial^\mu U^\dagger] + B_0 \mathrm{Tr}[(MU_0)U + (MU_0)^\dagger U^\dagger]$$

$$- c_1 \bar{N}((MU_0)P_L + (MU_0)^\dagger P_R)N$$

⇒ change nucleon mass

$$- c_2 \bar{N}(U^\dagger (MU_0)^\dagger U^\dagger P_L + U(MU_0)UP_R)N$$

change nucleon-pion interactions

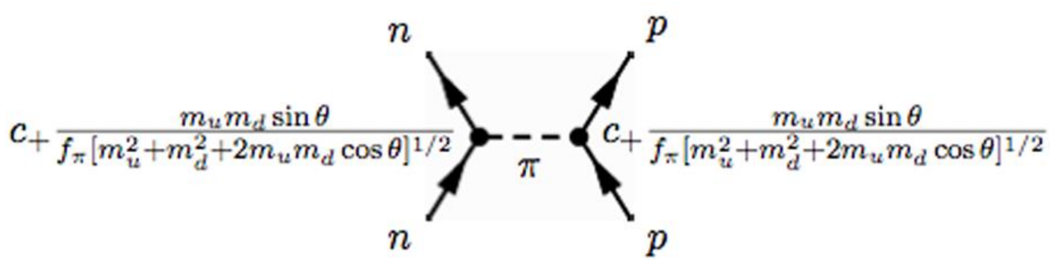

Simple example

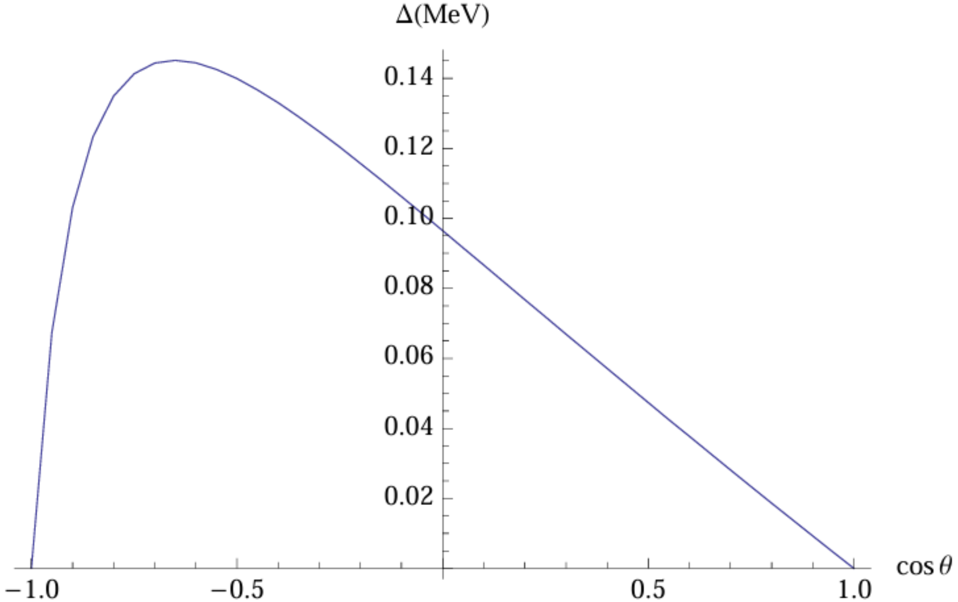

Figure 2: *Shift in the deuteron binding energy as a function of* $\cos\theta$

Mossbauer Effect

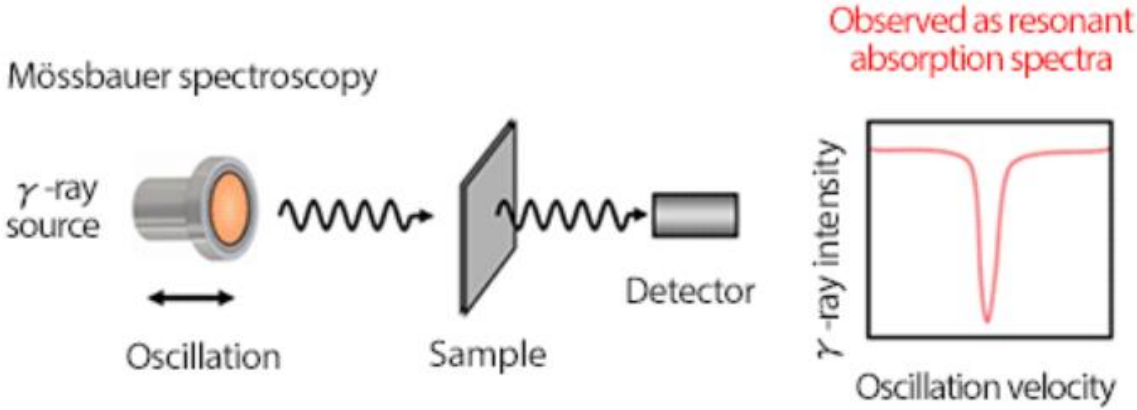

Ag-109 isotope
lifetime ~ 57s, $f \sim 88\ keV$ $\Rightarrow$ $\frac{\delta f}{f} \sim 10^{-22}$

It is very challenging to measure the natural linewidth experimentally.

So far, the best measurement has achieved 7 times of the nature width.

$$\frac{\delta f}{f} = g\,\Delta Z$$

($\Delta Z \rightarrow \mu m$)

If axion leads to the change of nucleon-pion coupling, it will change the energy splits.

Experiment Setup

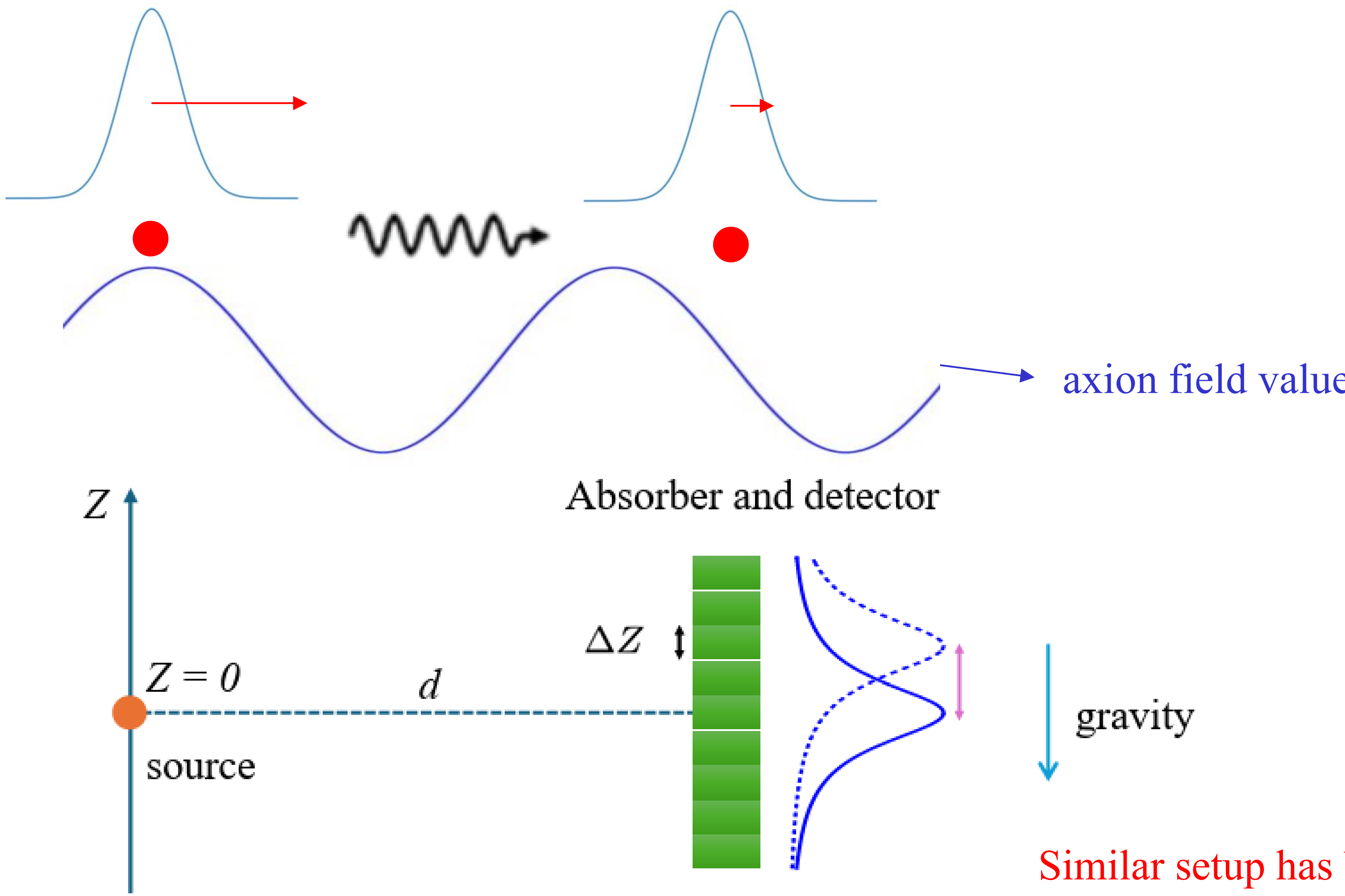

$$\delta E_{\mathrm{bind}}(d) = \Delta E_{\mathrm{bind}}(t+d, \vec{d}) - \Delta E_{\mathrm{bind}}(t, 0)$$

Similar setup has been proposed to search for gravitational wave.
Sci. Bull. 69, 2795 (2024)

Correction and Cancellation

assume related corrections
common factor
$(1 + \epsilon_{\alpha S}\, \theta^2)$

能量项	1/2⁻ (MeV)	7/2⁺ (MeV)	$\Delta E = E_{7/2^+} - E_{1/2^-}$
E_{α_S}	-17611.06	-17502.45	+108.61
E_{α_V}	13056.42	12985.91	-70.51
$E_{\alpha_{TV}}$	19.46	19.17	-0.29
E_{β_S}	2536.06	2508.91	-27.15
E_{γ_S}	-869.23	-856.75	+12.48
E_{γ_V}	-100.45	-99.36	+1.09
E_{δ_S}	46.32	44.55	-1.77
E_{δ_V}	196.86	189.64	-7.22
$E_{\delta_{TV}}$	2.20	2.13	-0.07
E_{kin}	1476.73	1461.69	-15.04
E_{cou}	333.96	334.49	+0.53
E_{pair}	-9.03	-10.49	-1.46
E_{Total}	-921.76	-922.57	-0.81

assume unrelated corrections

uncommon factor
$(1 + \epsilon_i\, \theta^2)$

$\delta E \sim (1 + \epsilon_{\alpha S}\, \theta^2)\, 100\ MeV$

Systematic and Statistical Uncertainties

$$N_{\rm det} = R_s \, {\rm Br} \, \delta T \frac{(2\pi d)\Delta Z}{4\pi d^2}$$

A too narrow detector leads to a very large statistical error.

source radiation intensity

branching ratio of the 88 keV photon

A competition:

the systematic uncertainty
worse with a larger detector width

the statistical uncertainty
better with a larger detector width

A smart data analysis strategy is introduced to balance these two competing aspects.

Sensitivity

	$g(g_\oplus)$	d(m)	ΔZ	ϵf_S	$m_{a,\max}$(eV)	R_s(Ci)
A	1	1	10μm	0.04	10^{-6}	1
B	10^{-4}	100	1 dm	0.04	10^{-6}	10

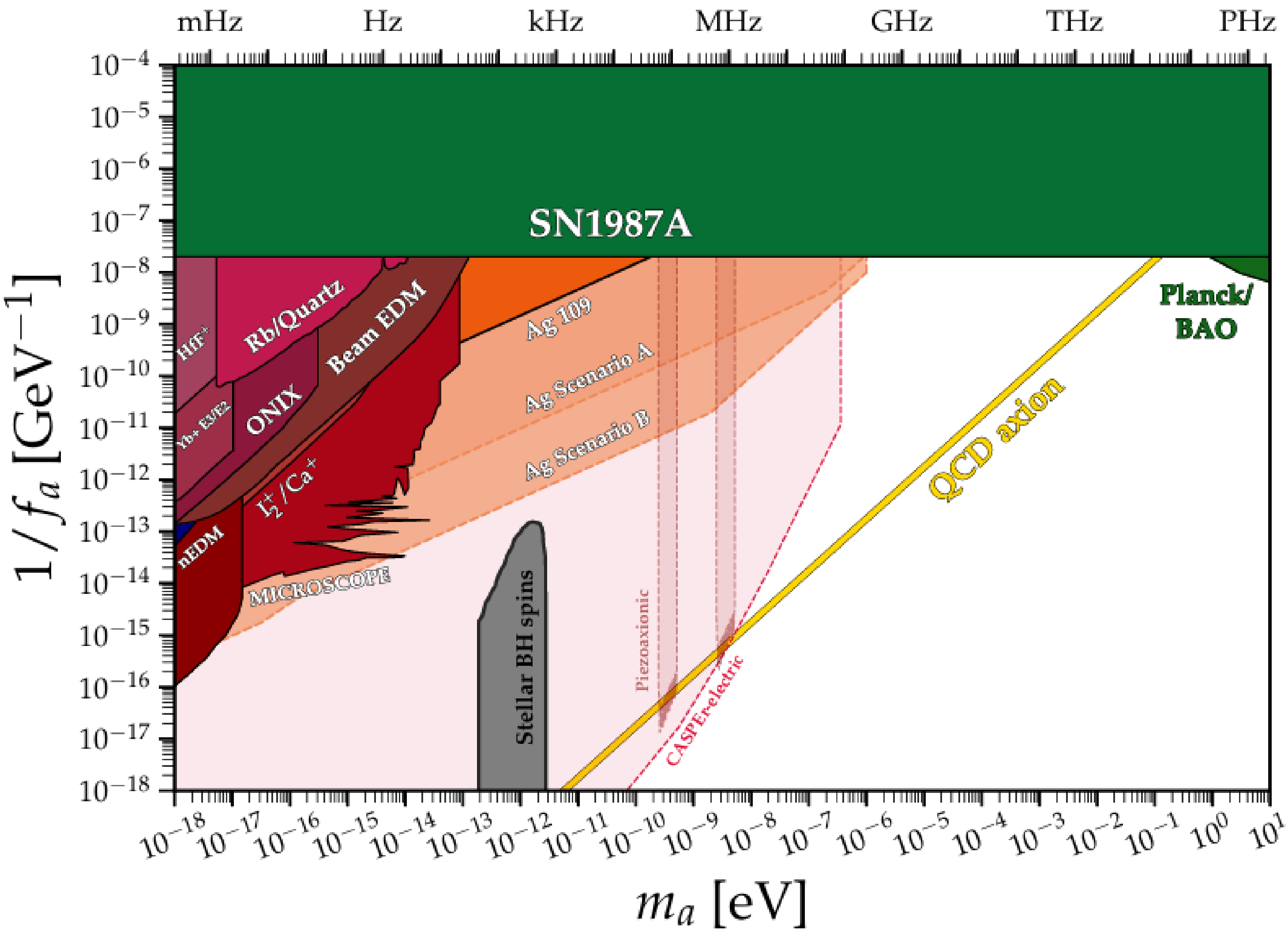

Sensitivity

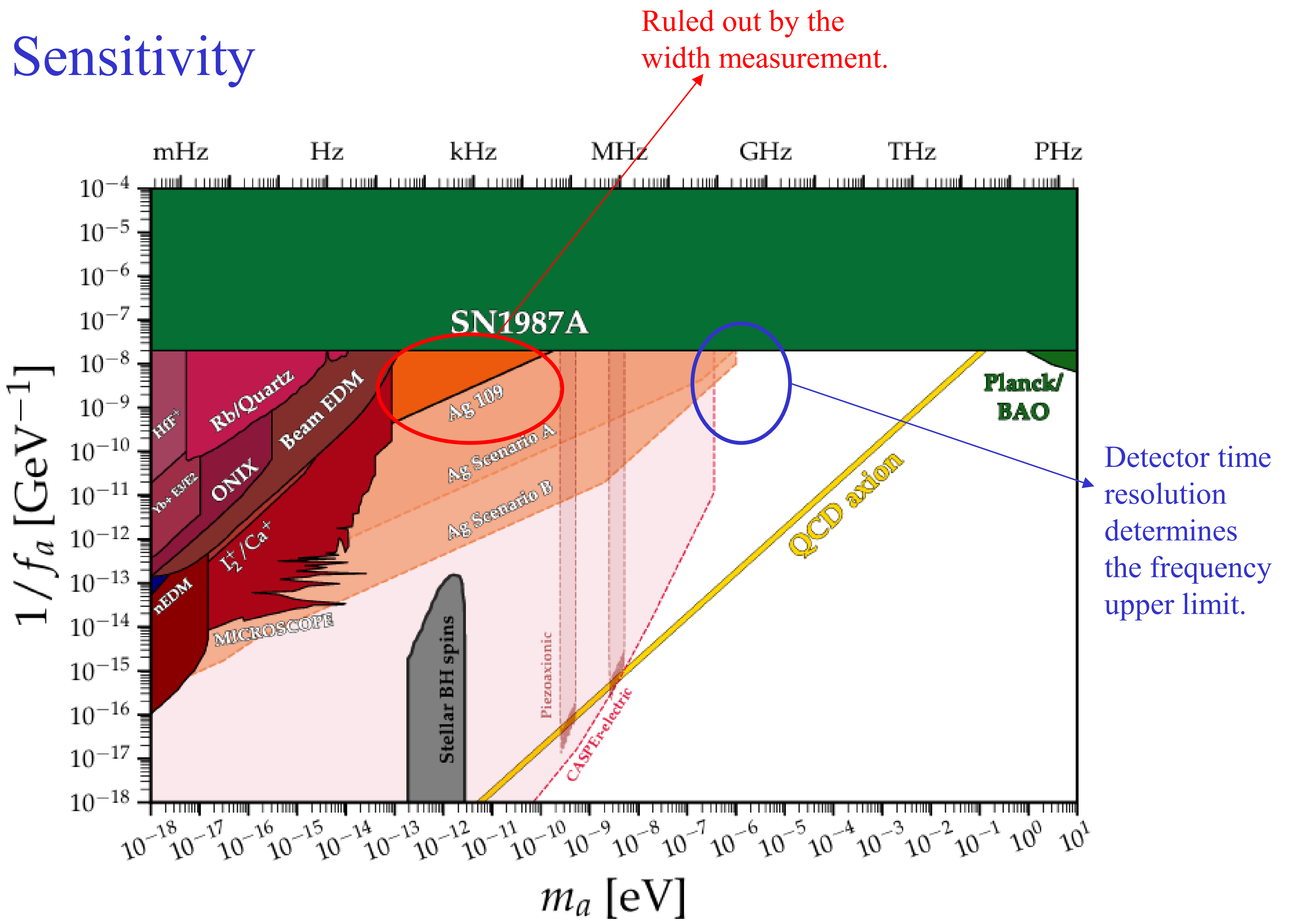

Conclusion 2

QCD axion dark matter leads to time-dependent nuclear binding energy.

This can be tested using Mossbauer Spectroscopy.

Ag-109 has an intrinsic width as 10^{-22}, perfect for this purpose.

Current width measurement has already imposed interesting constraints.

A large parameter space can be probed in the future.